NOTES AND CORRESPONDENCE

Bias in the Global Mean Temperature Estimated from Sampling a Greenhouse Warming Pattern with the Current Surface Observing Network

ROLAND A. MADDEN AND GERALD A. MEEHL

National Center for Atmospheric Research, Boulder, Colorado*

16 November 1992 and 26 April 1993

ABSTRACT

Theoretical and modeling studies suggest that increasing greenhouse gases will cause the global mean temperature to rise a few degrees centigrade during the next century. Current global coupled GCMs have shown a distinct pattern of warming associated with this global mean rise. It is important to know how well our observing network will be able to capture the global mean temperature rise associated with this pattern if it occurs. The authors consider if a sampling bias exists as a result of the spatial distribution of observations as they are now located (1950–1979) when detecting a pattern of temperature change that should be typical of a warming due to increasing atmospheric CO_2. The observations prove adequate to estimate the globally averaged temperature change associated with the pattern of CO_2 warming from a general circulation model with a bias whose absolute value is generally less than 2%.

1. Introduction

Estimates of global warming and climate sensitivity are typically given in terms of globally and annually averaged surface air temperature. However, the global warming signal generated by the current generation of global coupled GCMs is not homogeneous and has shown a distinct spatial pattern (IPCC 1992). Even if the existing observational network is adequate with respect to random errors (e.g., Folland et al. 1984; Jones et al. 1986a,b; Hansen and Lebedeff 1987) the question still arises whether or not it produces biases when sampling a specific anomaly pattern. The purpose of this note, therefore, is to determine if the current surface observing network is adequate to sample a specific pattern of surface air temperature change from increased CO_2, and to establish the size of biases, if they exist, in estimates of the globally averaged surface air temperature increase associated with that pattern.

We consider here only the bias that may arise due to imperfect spatial sampling. Imperfect temporal sampling can also cause bias (Trenberth et al. 1992). We assume that, on average, daily observations are randomly spaced within a month; that is, the expected value of daily observations within a month is the monthly mean at any given location. The location of observations are taken from the Global Monthly Surface Station Data Set (Shea and Spangler 1985) primarily based on observations from land stations and the Comprehensive Ocean–Atmosphere Data Set (Slutz et al. 1985), which consists of observations from ships of opportunity. The methodology is similar in most respects to that of a recent study of the random errors associated with estimating the global mean temperature in a long time series of model data (Madden et al. 1993).

2. CO_2 surface temperature signal

We don't know for certain what a temperature increase resulting from increasing atmospheric CO_2 (or other greenhouse gases) will look like, but coupled atmosphere–ocean simulations of the effect of increasing CO_2 generally agree that temperature increases should be largest in high northern latitudes, generally larger over land than over oceans, and smallest over the high-latitude southern oceans (Stouffer et al. 1989; Washington and Meehl 1989; Meehl et al. 1993; Cubasch et al. 1992; and summary by IPCC 1990, 1992).

A 60-year run of the NCAR R15 approximately 4.5° latitude by 7.5° longitude global coupled GCM with a linear increase in atmospheric CO_2 of 3.3 ppm yr^{-1} (Meehl et al. 1993) provides a plausible pattern of temperature increase with which we can test for bias in the imperfectly sampled means. Details of the model and basic experimental design are given in Washington and Meehl (1989). The control run and the transient experiment use an initial CO_2 concentration of 330 ppm. The differences between the increasing CO_2 run and a control run (constant CO_2) are shown in Fig. 9 of Meehl et al. (1993). They are based on annual means of the lowest model layer that are averaged over the

* The National Center for Atmospheric Research is sponsored by the National Science Foundation.

Corresponding author address: Dr. Roland A. Madden, NCAR, P.O. Box 3000, Boulder, CO 80307-3000.

last 30 years of the 60-year run. The temperature difference, or CO_2 signal, is positive all over the globe with largest values exceeding 1°C north of 60°N. When globally averaged, the CO_2 signal depicted in Meehl et al. Fig. 9 is 0.808°C. For our purposes this amplitude is arbitrary. Rather, we are most interested in the likely geographic distribution of the CO_2 signal. For convenience then, we multiplied the Meehl et al. values by 1.0/0.808 at each grid point so that the global average is 1°C. The result is shown in Fig. 1. The irregular curve in the right-hand panel of Fig. 1 is the area-weighted zonal mean temperature given by

$$T_{.,j} = \frac{1}{A} \sum_i T_{i,j} dA_j, \tag{1}$$

where $T_{i,j}$ is the temperature at the i, j grid point, and

$$dA_j = R^2(\Delta\lambda)W_j. \tag{2}$$

Here R is the radius of the earth, $\Delta\lambda$ is the longitudinal separation between grid points on the R-15 grid, and W_j is the Gaussian weight at latitude ϕ_j; A_j is the area of a latitudinal strip along ϕ_j or

$$A_j = \sum_i dA_j. \tag{3}$$

The total area (5.1×10^{14} m^2) is:

$$A = \sum_j A_j. \tag{4}$$

The sum of the $T_{.,j}$ over all latitudes is the global mean. That is

$$T_{.,.} = \sum_j T_{.,j} = 1°\text{C}. \tag{5}$$

The smooth line on the right hand side of Fig. 1 represents an area-weighted, homogeneous temperature increase of 1°C everywhere. The differences between the irregular and smooth curves simply reflect the fact that the zonal averages of the CO_2 signal, as well as the point values, are not homogeneous. It is the inhomogeneity in the Meehl et al. CO_2 signal that introduces the possibility of biases in the mean due to imperfect spatial sampling.

3. Sampling the temperature change pattern

To learn if the imperfectly sampled means might be biased when estimating the Meehl et al. CO_2 signal, Fig. 1 was sampled using

$$\hat{T}_{.,.} = \frac{1}{\hat{A}} \sum_i \sum_j T_{i,j}\delta_{i,j} dA_j, \tag{6}$$

where the $\hat{T}_{.,.}$ represents a spatial mean determined from the grid points that are near observations. The variable $\delta_{i,j} = 1$ if, during a given month, there was even a single observation near the grid point i, j. Otherwise $\delta_{i,j} = 0$. Also

$$\hat{A} = \sum_i \sum_j \delta_{i,j} dA_j. \tag{7}$$

An observation is near grid point i, j if it is within 389 km. This is a little less than half the longitudinal distance between grid points at the equator. Effectively an observation anywhere on the globe is assumed to be representative of an equal area of radius 389 km.

Figure 2 shows the mean temperature increase estimated from grid points near observations that existed from 1950 to 1979. There is an interesting annual vari-

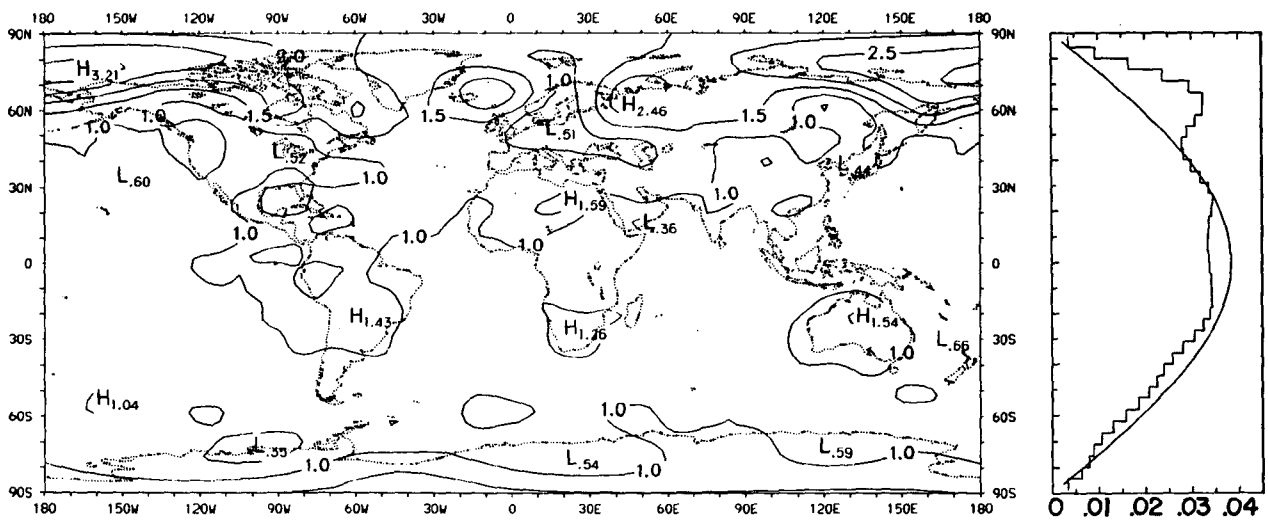

FIG. 1. Pattern of temperature increase caused by a linear increase in CO_2 in a global coupled general circulation model (after Meehl et al. 1993). Values are annual means averaged over the last 30 years of a 60-year run. They are scaled so that the area-weighted global mean is 1°C. The right-hand panel is the area-weighted zonal average of the GCM values (irregular line), and of a constant field of 1°C (smooth line).

ation in the estimates with, after 1951, northern summertime estimates biased warm (true temperature change is 1°C) and wintertime estimates biased cold. In both cases the bias tends to be less than 2%. The cause of the annual variation in the bias is an annual variation in the location and number of observations. This is reflected in the percent area observed, which has seasonal change of about 6% with maximum in northern winter.

Figure 3 shows the percent area observed during January and July averaged over the 1950–1979 period as a function of latitude. The seasonal changes are relatively small north of 40°S. The biggest seasonal change occurs over the southern oceans from 40° to 70°S. There, a minimum of observations is available during July. This seasonal variation affected the IGY (1957/1958) World Weather Map Project as noted by Taljaard and van Loon (1964); ". . . but as in other years ships were rare south of the 40th parallel from April until late November," and was still a factor in the late 1970s. During northern winter when there are more observations over the southern latitudes, this relatively cool (less warm) region (which is consistent in all the coupled models run with transient CO_2 increases—see IPCC 1992) contributes more to the area-weighted mean and to the cold bias. On the other hand, during northern summer, when there are fewer observations over the relatively cool southern latitudes, they contribute less to the area-weighted mean, resulting in a warm bias.

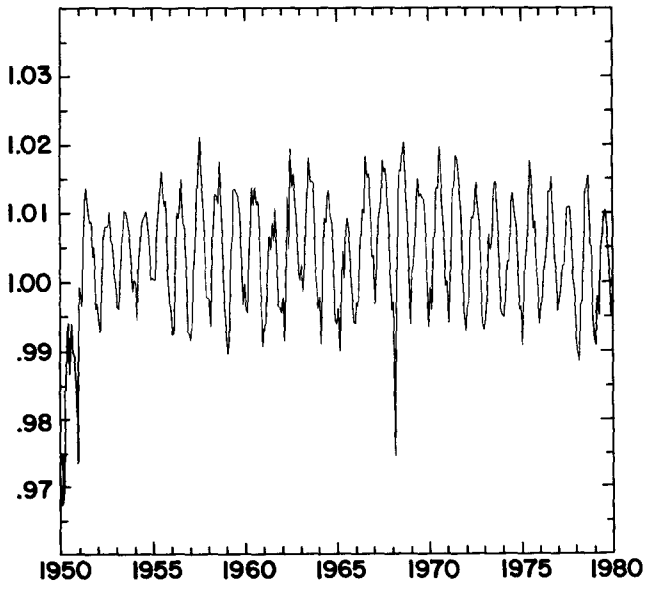

FIG. 2. Area-weighted global averages of Fig. 1 determined by (6) using only grid points near actual observations as they existed each month from January 1950 through December 1979. The true mean is 1°C. After 1950 (6) gives values less (more) than 1°C during northern winter (summer).

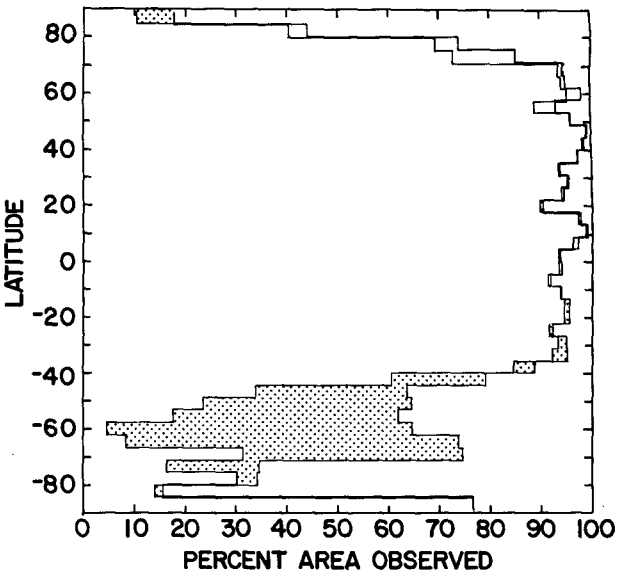

FIG. 3. Average (1950–1979) percent area observed as a function of latitude during January (thick line) and July (thin line). Stippled area represents additional coverage in January over July.

4. Conclusions

We conclude that the spatial distribution of observations of the surface temperature available since the 1950s results in a bias of less than 2% when estimating the global annual CO_2 warming from the specific annual mean spatial pattern of surface temperature change from Meehl et al. This pattern, while not certain, is typical of those generated by coupled atmosphere–ocean simulations of the effect of increasing CO_2. Figure 3 suggests a seasonal effect due primarily to changes in the number of available observations in the southern oceans. At the same time, the seasonal cycle in the CO_2 signal, which we have not attempted to deal with, is thought to be large at high northern latitudes and small in high southern latitudes (Washington and Meehl 1989; IPCC 1992). As a consequence, this small bias suggested for the model's annual mean signal should be reasonably representative in spite of seasonal variations in the signal. This is so because the seasonal variation of the signal is expected to be small where the seasonal variation of the observations is largest (high southern latitudes).

REFERENCES

Cubasch, U., K. Hasselmann, H. Hock, E. Maier-Reimer, W. Mikolajewicz, B. D. Santer, and R. Sausen, 1992: Time dependent greenhouse warming computations with a coupled ocean-atmosphere model. *Climate Dyn.*, **8**, 55–69.

Folland, C. K., D. E. Parker, and F. E. Kates, 1984: Worldwide marine temperature fluctuations 1856–1981. *Nature*, **310**, 670–673.

Hansen, J., and S. Lebedeff, 1987: Global trends of measured surface air temperature. *J. Geophys. Res.*, **92**, 13 345–13 372.

IPCC, 1990: *Climate Change: The IPCC Scientific Assessment.* J. T. Houghton, G. J. Jenkins, and J. J. Ephraums, Eds., Cambridge University Press, 365 pp.

IPCC, 1992: *Climate Change 1992: The supplementary report to the IPCC Scientific Assessment.* J. T. Houghton, B. A. Callander, and S. K. Varney, Eds., Cambridge University Press, 200 pp.

Jones, P. D., S. C. B. Raper, R. S. Bradley, H. F. Diaz, P. M. Kelly, and T. M. L. Wigley, 1986a: Northern Hemisphere surface air temperature variations, 1851–1984. *J. Climate Appl. Meteor.,* **25,** 161–179.

——, S. C. B. Raper, and T. M. L. Wigley, 1986b: Southern Hemisphere surface air temperature variations: 1851–1984. *J. Climate Appl. Meteor.,* **25,** 1213–1230.

Madden, R. A., D. J. Shea, G. W. Branstator, J. J. Tribbia, and R. Weber, 1993: The effects of imperfect spatial and temporal sampling on estimates of the global mean temperature: Experiments with model data. *J. Climate,* **6,** 1057–1066.

Meehl, G. A., W. M. Washington, and T. R. Karl, 1993: Low-frequency variability and CO_2 transient climate change. Part 1: Time-averaged differences, *Climate Dyn.,* **8,** 117–133.

Shea, D. J., and W. L. Spangler, 1985: NCAR's Global Monthly Surface Station Data Set Preprints, *Third Conference on Climate Variations: Symposium on Contemporary Climate: 1850–2100,* Los Angeles. Amer. Meteor. Soc., 12–13.

Slutz, R. J., S. J. Lubker, J. D. Hiscox, S. D. Woodruff, R. L. Jenne, D. H. Joseph, P. M. Steurer, and J. D. Elmo, 1985; COADS: The Comprehensive Ocean-Atmosphere Data Set. Release 1. Climate Research Program, ERL/NOAA, Boulder, CO, 39 pp. [NTIS No. PB86-105723.]

Stouffer, R. J., S. Manabe, and K. Bryan, 1989: Interhemispheric asymmetry in climate response to a gradual increase of atmospheric CO_2. *Nature,* **342,** 660–662.

Taljaard, J. J., and H. van Loon, 1964: Southern Hemisphere weather maps for the International Geophysical Year. *Bull. Amer. Meteor. Soc.,* **45,** 88–95.

Trenberth, K. E., J. R. Christy, and J. W. Hurrell, 1992: Monitoring global monthly mean surface temperatures, *J. Climate,* **5,** 1405–1423.

Washington, W. M., and G. A. Meehl, 1989: Climate Sensitivity due to increased CO_2. Experiments with a coupled atmosphere and Ocean general circulation model. *Climate Dyn.,* **4,** 1–38.